IJE TRANSACTIONS A: Basics Vol. 35 No. 10, (October 2022) 1967-1980

International Journal of Engineering

Journal Homepage: www.ije.ir

# Glutaraldehyde: Introducing Optimum Condition for Cross-linking the Chitosan/Gelatin Scaffolds for Bone Tissue Engineering

F. Banafati Zadeh, A. Zamanian*

*Department of Nanotechnology and Advanced Materials, Materials and Energy Research Center, Karaj, Iran*

*PAPER INFO*

*Paper history:*
Received 24 January 2022
Received in revised form 18 May 2022
Accepted 15 June 2022

*Keywords*:
*Bone Tissue Engineering*
*Chitosan*
*Cross-linking*
*Gelatin*
*Glutaraldehyde*

*ABSTRACT*

Large bone defects caused by trauma or disease needs extra intervention. Gelatin/chitosan complex is one of the most valuable compositions for bone healing, but fast degradation in aqueous solution and low mechanical properties increase the need for cross-linking agent. The cross-linker concentration and cross-linking method had a significant effect on the properties of fabricated scaffolds. Here, three different cross-linking methods of Glutaraldehyde (GA), including addition to the solution, vapor exposure, and immersion, were studied by different in-vitro analyses to find the best GA cross-linker concentration and cross-linking method. Scanning electron microscopy showed homogeneous microstructures in all samples. Fourier transform infrared spectrophotometry revealed cross-linking reactions in all samples. Swelling ratio and biodegradation ratio was reduced by increasing cross-linking concentration and exposure time. Nonetheless, higher cross-linker concentration and exposure time improved mechanical properties, while it seems the cross-linking exposure time had more effect than concentration. Accordingly, GA (1 wt%) cross-linked scaffold with solution addition method showed suitable performance with 39.3° contact angle, 1.45±0.05 MPa compressive strength, 22.31±1.3 (%) swelling ratio, and 26.33±4.47 (%) biodegradation ratio. In-vitro experiments indicated cells were spread all over the scaffolds with higher than 80 (%) cell viability in all time points. The expression of alkaline phosphatase (ALP) and osteo-related genes (osteocalcin and related transcription factor 2) were improved during 14 days of cell incubation and showed the high capacity of the scaffold support in mineralization and osto-differentiation. Therefore GA (1 wt% ) cross-linked scaffold with solution addition was introduced as the best candidate for bone repair and further studies.

***doi***: *10.5829/ije.2022.35.10A.15*

## 1. INTRODUCTION

The growing older population increased the need for bone replacement all around the world [1]. Bone is known as the most frequently transplanted organ after blood [2]. Large bone defects cannot be regenerated naturally and required external intervention [3, 4]. Drawbacks of autografts and allografts such as additional defect sites, low number of donors, and disease transmission limited their usage and introduced tissue engineering as a novel proper substitution [5]. Tissue engineering combines cell, scaffolds, and biological factors to mimic the defect site's extracellular matrix (ECM) [6, 7].

A favorable scaffold should be biocompatible, biodegradable, highly porous with interconnected pores for nutrition and oxygen flow with sufficient mechanical strength, and provide a suitable microenvironment for cell adhesion, proliferation, and growth [8, 9]. To date, several polymers have been used for different biomedical applications and the fabrication of bone tissue engineering scaffolds [10-15]. Chitosan, a biocompatible, biodegradable natural polysaccharide derived from chitin of crustaceans exoskeletons, has gained a lot of attention in tissue engineering [16]. The advantage of chitosan, such as biocompatibility, biodegradability, antibacterial properties, and non-toxicity, made it popular for bone tissue engineering and drug delivery [17-19]. However, chitosan cannot provide

*Corresponding Author Institutional Email: a-zamanian@merc.ac.ir (A. Zamanian)

Please cite this article as: F. Banafati Zadeh, A. Zamanian, Glutaraldehyde: Introducing Optimum Condition for Cross-linking the Chitosan/Gelatin Scaffolds for Bone Tissue Engineering, ***International Journal of Engineering, Transactions A: Basics***, Vol. 35, No. 10, (2022), 1967-1980

a suitable mimicked-substrate for cell functionalization; accordingly, composite structure fabrication can compensate for this problem. Therefore, gelatin, a natural and water-soluble biopolymer that is obtained from the denaturation of collagen [20, 21], can be the suitable choice for fabrication of regenerative bone substitutes due to the presence of Arg-Gly-Asp (RGD)-like sequences which can enhance cell adhesion and proliferation [22].

Although chitosan/gelatin composition has been previously used as the scaffold compound in bone tissue engineering applications [23], it should be cross-linked before usage to enhance mechanical and chemical stability as well as long-lasting the scaffolds [20]. Cross-linking is chemical or physical bonds between polymer chains to modify mechanical, biological, and degradation properties [24]. There are different techniques typically in three physical, chemical, enzymatic categories for cross-linking chitosan and gelatin [25]. The physical cross-linking revealed some drawbacks such as low cross-linking degree and mechanical properties. Lee et al. [26] used e-beam physical cross-linking, while the higher e-beam dose reduced the molecular weight and as a result decreased previous cross-linking effects. Furthermore, it was not satisfying in bulk gelatin samples. In addition, enzymatic cross-linking may show low cross-linking efficiency. Chemical agents addition is the most often method among the mentioned methods due to its easiness and high output crosslinking [27, 28]. As a result, here we used chemical cross-linking manner of gelatin and chitosan. Among different kinds of gelatin and chitosan cross-linkers, glutaraldehyde (GA) is one of the most popular cross-linkers due to its inexpensive, availability, and high efficiency [29]. Cross-linking chitosan and gelatin with GA is very efficient because of the large number of the amine and hydroxyl groups in their chemical composition [30]. Different kinds of cross-linking manners suggested for GA such as solution addition [31], vapor [32], and immersion [33]. Badawy et al. [20] added different concentrations of GA to chitosan/alginate/gelatin gel spheres. Higher GA concentration formed more rigid constructs with lower swelling capacity. The other cross-linking method is vapor cross-linking, which is one of the favorable methods due to its easy control and inhibiting structure collapsing of the scaffolds [34]. Zhu et al. [34] used GA vapor for cross-linking carboxyethyl chitosan and polyvinyl alcohol scaffolds. Their results demonstrated that the constructs' stability improved after vapor cross-linking while maintaining their high cell viability. In another study, the freeze-dried scaffolds were soaked in 1 wt.% GA for cross-linking followed by deionized water immersion to remove the extra amount of GA. The cellular and mechanical investigations revealed that GA cross-linked gelatin/chitosan/nanobioglass had proper durability with favorable cellular adhesion [35, 36].

Although several articles have been presented on the cross-links of gelatin and chitosan, as far as we know, there is no reference article comparing different cross-linking methods when using GA for bone tissue engineering applications and the need for a comprehensive article to examine and compare cross-linkers concentration and cross-linking method is felt. In this study, biocompatible gelatin/chitosan scaffolds fabricated by freeze-drying technique and the effect of cross-linker concentration and three different GA cross-linking methods (solution addition, vapor cross-linking, and cross-linking immersion) on gelatin/chitosan scaffolds have been investigated. For this, the effect of cross-linker on the morphological and pore size was evaluated. Then, the chemical interactions, swelling, degradation, and mechanical behavior of each scaffold were studied. Contact angle measurement was conducted on the selected scaffold with more favorable properties for bone tissue replacement. Finally, optimum GA cross-linked scaffolds' capacity for cell adhesion, proliferation, and differentiation was studied.

## 2. MATERIALS AND METHODS

**2. 1. Aterials** Gelatin ($M_w$ =40–50 KDa), glutaraldehyde (25%, d = 1.058 g/cm$^3$), ethanol ($M_w$=46.07 g/mol), and acetic acid ($M_{w=}$ 60.05 g/mol) were purchased from Merck Co. Ltd. (Darmstadt, Germany). Chitosan ($M_w$= 190–310 kDa, DD=75– 85%), thiazolyl blue tetrazolium bromide (MTT, $M_w$= 414.32 g/mol), p-nitrophenyl phosphate (pNPP, tablet), and dimethyl sulfoxide (DMSO, 1X) were purchased from Sigma Co. Ltd. (Massachusetts, USA). Phosphate buffer saline powder (PBS, pH 7.2– 7.4) was purchased from Aprin advanced technology development Co. Ltd. (Tehran, Iran). Alkaline phosphatase kit (ALP) was purchased from MAN Co. Ltd. (Tehran, Iran). Dulbecco's Modified Eagle's medium (DMEM), fetal bovine serum, penicillin-streptomycin were purchased from Gibco-BRL, Life Technologies Co. Ltd. (N.Y., USA). All the chemicals were analytical grade and were used without any purification. All aqueous solutions were prepared with deionized (DI) water.

**2. 2. Fabricating of GA Cross-linked Scaffolds** To prepare chitosan/gelatin (2 wt.%) solution, chitosan powder (3g) was added to the acetic acid (2 M, 300 ml) under the stirring condition at 35 ℃ for 24 h. Then, gelatin (3g) was added to the solution under stirring conditions, and stirring was continued for 5 h at 35 ℃ to prepare a homogenous solution.

In order to fabricate GA cross-linked scaffolds, three cross-linking manners (solution addition, immersion, and vapor) were applied. For solution addition GA cross-linking, 0/5 and 1 (wt.%), GA was added to 30 ml

chitosan/gelatin solution under stirring condition for 0.5 h to obtain a homogeneous solution. Then, the cross-linked contained solution was transferred to the freeze-drier. For this purpose, the as-prepared solutions (contained or non-contained cross-linking agent**)** were poured into aluminum cylinders made of aluminum sheets with a diameter of 1.0 mm and height of 170 mm and kept at -20 ℃ for 24 h then freeze-dried at -50 ℃ and 0.5 torr for 48 h (Pishtaz Equipment Engineering co., Iran). The freeze-dried samples were then cut as discs with 10 mm in diameter and 15 mm in height.

For vapor and immersion cross-linking, the prepared gelatin-chitosan solution was freeze-dried to create chitosan/gelatin scaffolds at the first step. The applied freeze-drying conditions were the same as the earlier mentioned conditions. Then, some cross-linker free scaffolds were selected for GA vapor cross-linking and moved to a sealed desiccator containing 10 ml of 25% aqueous GA solution in a Petri dish. The scaffolds were placed on a shelf in the desiccator in the exposure of GA vapor for 6, 24, and 48 h at room temperature. After cross-linking, the cross-linked scaffolds were placed in a hood for 2 h followed by deionized water soaking at 37◦C for 1 day. The final scaffolds were dried at 60°C for 24 h.

The other freeze-dried scaffolds were cross-linked by GA immersion. So, the scaffolds were immersed in 0.5, 1, and 2 wt. % GA solution for 1 and 24 h at 37 °C. Then, the scaffolds were washed with deionized water for 2 min followed by 1 h immersion in ethanol for unreacted GA removing. The samples were dried at room temperature for 24 h. The prepared sample codes were summarized in Table 1.

**TABLE 1.** The compositions of fabricated scaffolds

| Code | Base | GA Concentration (wt. %) | Method | Time (h) |
|---|---|---|---|---|
| Control | 2.0 wt.% chitosan/gelatin | ---- | ---- | - |
| GA0.5S | | 0.5 wt. % | Adding to the solution | 0.5 |
| GA1S | | 1 wt. % | Adding to the solution | 0.5 |
| GAV-6 | | 25 wt. % | Vapor | 6 |
| GAV-24 | | 25 wt. % | Vapor | 24 |
| GAV-48 | | 25 wt. % | Vapor | 48 |
| GA0.5I-1 | | 0.5 wt. % | Immersion | 1 |
| GA0.5I-24 | | 0.5 wt. % | Immersion | 24 |
| GA1I-1 | | 1 wt. % | Immersion | 1 |
| GA1I-24 | | 1 wt. % | Immersion | 24 |
| GA2I-1 | | 2 wt. % | Immersion | 1 |
| GA2I-24 | | 2 wt. % | Immersion | 24 |

## 2. 3. Characterization

**Morphology observations:** The morphology of the fabricated scaffolds was observed using scanning electron microscopy (SEM, Vega, Czech Republic) at an accelerating voltage of 5 kV. A thin layer of gold was coated on the samples before SEM observation.

**Fourier transform infrared spectroscopy (FTIR):** In order to investigate the chemical functional groups of the prepared scaffolds, FTIR spectroscopy was performed. Therefore, a Perkin-Elmer Spectrum 400 Fourier transfer infrared (FTIR) spectrophotometer in the wavenumber range of 400–4,000 $cm^{-1}$ was used.

**Water-scaffold interactions:** The swelling (water absorption) capacity of the prepared scaffolds was calculated using Equation (1) after immersion of the round samples for 5, 30, 60, 120 min in 15 ml in the PBS solution at 37 ± 0.5 °C [37]:

$$Absorption(\%) = \left|(W_w - W_d)/W_d\right| \times 100 \quad (1)$$

where $W_d$ is the weight of the dried scaffold and $W_w$ is the weight of the scaffold after being placed in PBS. The test was repeated on five samples and the average result was reported.

**Biodegradation ratio**: The biodegradation ratio of the prepared scaffolds was calculated using Equation (2) after soaking of the scaffolds for 2 weak in phosphate-buffered saline (PBS) at 37 ± 0.5 °C [38]:

$$\text{Biodegradation}(\%) = \left|(W_w - W_d)/W_d\right| \times 100 \quad (2)$$

where $W_w$ is the initial weight of the scaffold (before immersion in PBS) and $W_d$ is the weight of scaffold after immersion in PBS. The test was repeated on five samples and the average result was reported.

**Mechanical strength**: The Mechanical properties of the scaffolds were measured by a compression strength test system (Santam, STM 20, Iran) with a crosshead speed of 0.5mm/min. All the specimens were cut into 10 mm [39]. The test was repeated on five samples and the average result was reported.

**Contact angle:** In addition, the wettability of the selected scaffolds was analyzed by water contact angle measurements. The sessile drop method (Kruss DSA 100, Germany) used the water contact angle assay at room temperature. The droplet size was set to 1.0 ml [40]. The test was repeated on five samples and the average result was reported.

## 2. 4. Cells-Scaffold Interactions

**Cell morphology:** Adhered cell morphology observation investigated the capability of the optimum scaffolds to cell attachment. So, $5\times10^4$ cells/ml (rat bone marrow mesenchymal stem cells (BMSCs, supplied by Fudan University Hospital Medical Center) were seeded on the surfaces of each sterilized scaffolds, and DMEM with 15% (v/v) FBS and 100 mg/ml penicillin-streptomycin

were added to each well. The cells were incubated for 3 days at 37 ± 0.5 °C and 5 % $CO_2$. After 3 days, the DMEM was removed, and each sample was washed by PBS solution. The fixation was performed by glutaraldehyde and 1 % osmium tetroxide. The ascending ethanol concentration (10, 30, 50, 79, 90, 95, and 100) was added to each sample for dehydration. After drying in air condition, the morphology of adhered cells was observed by FE-SEM.

**MTT:** Viability of the cells was obtained 2, 4, and 7 days after cell culture. MTT test was conducted with L929 fibroblast cells. After determined time points of cell cultures, the DMEM was removed and was replaced by fresh 10 μ L MTT contained culture medium. The cells were incubated by a fresh medium. After 2 h incubation at 37 °C with 5% $CO_2$, the culture medium and MTT were removed, and 100 μl of DMSO was added to each well plate. The optical density was measured at 570 nm wavelength [41, 42]. The cell viability was calculated using the Equation (3).

$$Cell Viability\ (\%) = (ODsample / ODcontrol) \times 100 \quad (3)$$

**Alkaline phosphatase (ALP) assay:** In order to determine the ALP activity as an indicator of osteo-differentiation, p-nitrophenol from p-nitrophenyl phosphate (p-NPP) releasing level was measured after 0, 7, and 14 days of cell culture. Lysing was performed by the addition of 0.1 % Titron X-100 followed by freeze-thawing at 37±0.5°C. ALP level was determined using ALP kit, so the reaction was stopped by NaOH (1N), and the absorbance was investigated at 405 nm [43].

**Cell differentiation:** The expression level of Osteogenic-related genes such as osteocalcin (OC) and runt-related transcription factor 2 (RUNX2) was evaluated using Real-time (RT) polymerase chain reaction (PCR). For this purpose, BMSCs cells were cultured for 72 h on the surface of the scaffolds. Then, the osteogenic medium was replaced, and cells were cultured for 7 and 14 days. Every 2 days, the osteogenic medium was refreshed. At the end of each time point (0, 7, and 14 days), the total RNA was extracted using TRIzol Reagent (Invitrogen Pty Ltd, Australia). cDNA was synthesized from the RNA of each sample by SuperScript II First-Strand cDNA synthesis kit. The relative gene expression was calculated at 95 °C for 3 min followed by 40 cycles of 95 °C for 3 s and 60 °C for 30 s using specific primers. OC: Forward, GGGAGACAACAGGGAGGAAAC; Reverse, TCGGTCATGCTCTCTCCAAAC. RUNX2: Forward, CCCAGCCACCTTTACCTACA; Reverse, TATGGAGTGCTGCTGCTGGTCTG. Results normalized with housekeeping gene GAPDH as a control. GAPDH: Forward, GCCCAATACGACCAAATCC; Reverse, AGCCACATCGCTCAGACA. All the cell investigations were repeated on five samples and the average result was reported.

**2. 5. Statistical Analyzes** The results were presented as the mean ± standard deviation of 5 experiments using Microsoft Excel 2016 software (Microsoft, Redmond, WA, USA). Statistical analysis was performed by using one-way ANOVA and Tukey test with significance reported when $P < 0.05$.

## 3. RESULTS AND DISCUSSION

**3. 1. Morphology Observation** Figures 1 and 2 demonstrate the SEM micrographs and pore size distribution of prepared scaffolds with different concentrations of GA and various cross-linking methods. As can be seen, the open pores are uniformly formed, and thin walls separate the pores in all samples. Figures 1(a) and (b) shows SEM micrographs of GA0.5S and GA1S samples, respectively, Figure 1 (c-e) indicates the SEM micrographs of GAV-6, GAV-24, and GAV-48 scaffolds, respectively, and Figure 1(f) presents mean pore size. The pore size samples were in the range of 50-400 μm. Here, GA0.5S and GA1S showed the average pore diameter of 233.00±7.64 and 140.16±5.64 μm, respectively. But pore size of the GAV-6, GAV-24, and GAV-48 scaffolds was calculated 232.41±8.43, 187.14±7.7, and 75.26±5.56 μm, respectively. Figure 2 (a-f) shows the SEM micrographs of GA0.5I-1, GA0.5I-24, GA1I-1, GA1I-24, GA2I-1, and GA2I-24, respectively. Figure 2(g) demonstrate the average pore size of GA immersion cross-linked samples. Here, the pore diameter mean was calculated 160.95±7.02, 154.92±6.9, 160.31±6.9, 99.25±3.28, 141.26, and 72.78±29.92 μm for GA0.5I-1, GA0.5I-24, GA1I-1, GA1I-24, GA2I-1, and GA2I-24, respectively. All GA cross-linked samples with different methods such as vapor, immersion, and solution addition, exhibited porosity between 20-80%. In the case of pore size, increasing the cross-linking time and concentration decreased the average pore size in all samples.

As a critical parameter for biomedical applications, the microstructure of the scaffolds should provide the suitable geometry for better cell migration, cellular proliferation, and proper vascularization for transportation of nutrients and removal of waste products [44]. According to the morphology observations and average pore size of samples cross-linked by the GA immersion method, a more irregular pore shape was observed than other scaffolds. It should be noted that although these samples had more scattered values, the average pore diameter of all GA immersed samples was in the range of 50-200 μm. The optimum pore size for BMSCs growth was found to be in the range of 100-500 μm, which can be approximately matched with the pore

size range in prepared GA cross-linked scaffolds [45, 46]. Small pores restrict cell migration and infiltration into the 3D structure of the scaffolds, while large pores with better cell responses reduce the mechanical properties [47]. Accordingly, a range of small and large pores is required for observing better results, as achieved in currently modified scaffolds. A proper bone tissue engineering scaffold should have porosity in the range of 20-90 % depends on the cortical and cancellous bone structure [48]. The all samples had porosity in the mentioned range. However, pore sizes were in the range of 50-400 µm which were in the proper range for bone replacement [45, 46]. The pore size results demonstrated that the GA vapor cross-linked scaffolds had a primarily homogenous morphology. The samples cross-linked by GA vapor exposure had a more uniform structure than samples cross-linked with other methods. Although there was slight pore morphology deformation, the pores were still open with suitable size, and this change can be negligible.

**3. 2. Fourier Transform Infrared Spectroscopy (FTIR)** FTIR spectroscopy investigated the chemical composition of the freeze-dried scaffolds, and the results are demonstrated in Figures 3(a)-(c). Chitosan/gelatin scaffolds without any cross-linker were considered as the control sample. The characteristic peaks of chitosan and gelatin were detected in all FTIR samples. The wide absorption band at around 3100-3600 $cm^{-1}$ was attributed to the stretching vibration of O-H bonded to N-H in all samples [49]. The specific chitosan peaks were

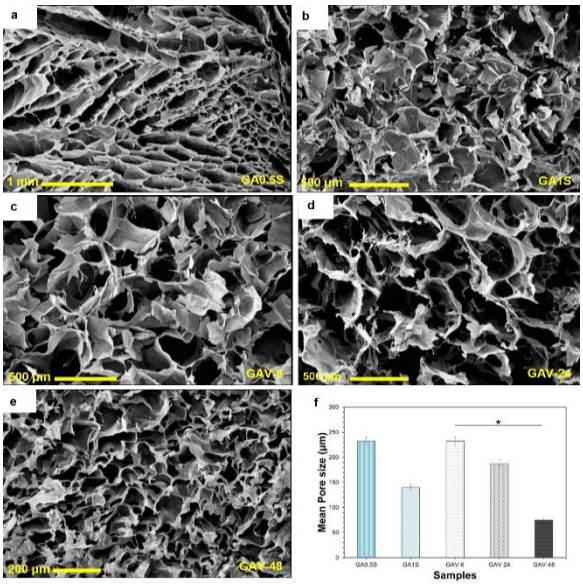


**Figure 1.** SEM micrographs of (a) GA0.5S; (b) GA1S; (c) GAV-6; (d) GAV-24; (e) GAV-48 scaffolds. (f) The mean pore size measurements of GA0.5S, GA1S, GAV-6, GAV-24, and GAV-48 scaffolds

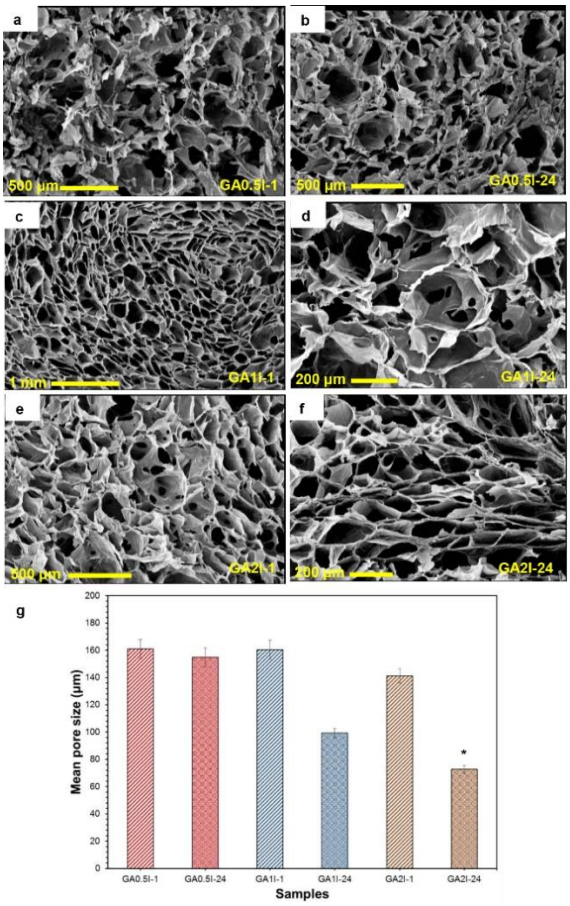


**Figure 2.** SEM micrographs of (a) GA0.5I-1; (b) GA0.5I-24; (c) GA1I-1; (d) GA1I-24; (e) GA2I-1; (f) GA2I-24 scaffolds. (g) The mean pore size measurements of GA0.5I-1, GA0.5I-24, GA1I-1, GA1I-24, GA2I-1, and GA2I-24 scaffolds

detected at around 1651 $cm^{-1}$, 1542 $cm^{-1}$, and 1381 $cm^{-1}$, due to C=O stretching (amide I), N-H bending (amide II), and N-H bending and C-N stretch (amide III), respectively [50]. Figure 4(a) illustrates the proposed schematic of GA cross-linking reaction process of chitosan and gelatin using solution addition (a), vapor exposure (b), and immersion (c) methods, respectively, and Figure 4(b) shows the schematic of cross-linking techniques for chitosan/gelatin scaffolds.

Chitosan/gelatin crosslinking mechanism by GA has been performed through nucleophile addition-type reaction by the aldehyde functional groups with free non-protonated ε-amino groups of chitosan and gelatin reactions [51]. GA cross-linking created covalent linkage imine bonds (-C=N) between aldehyde groups of GA and amine group of gelatin and chitosan at around 1651 $cm^{-1}$ and merged with amid I bonds of gelatin and chitosan [52]. Amine-containing compounds such as polysaccharides can easily react with aldehyde functionalities such as used GA here and create Schiff base compound [53], also this Schiff base mechanism

was demonstrated in a previous study by Patel et al. [54]. According to the achieved FTIR results, the higher GA cross-linker or higher exposure time intensified C=N related peak and confirmed the higher cross-linking percentage of chitosan and gelatin. These results were incontinence with a previous study performed by Nguyen et al. [31]. Accordingly, GA was considered a creep cross-linking, and in the early hours, GA could not completely cross-linked gelatin and chitosan due to the environment's acidity. However, the acid had been evaporated during the time, and as a result, the cross-linking process of the sample was better performed in samples with higher immersion time.

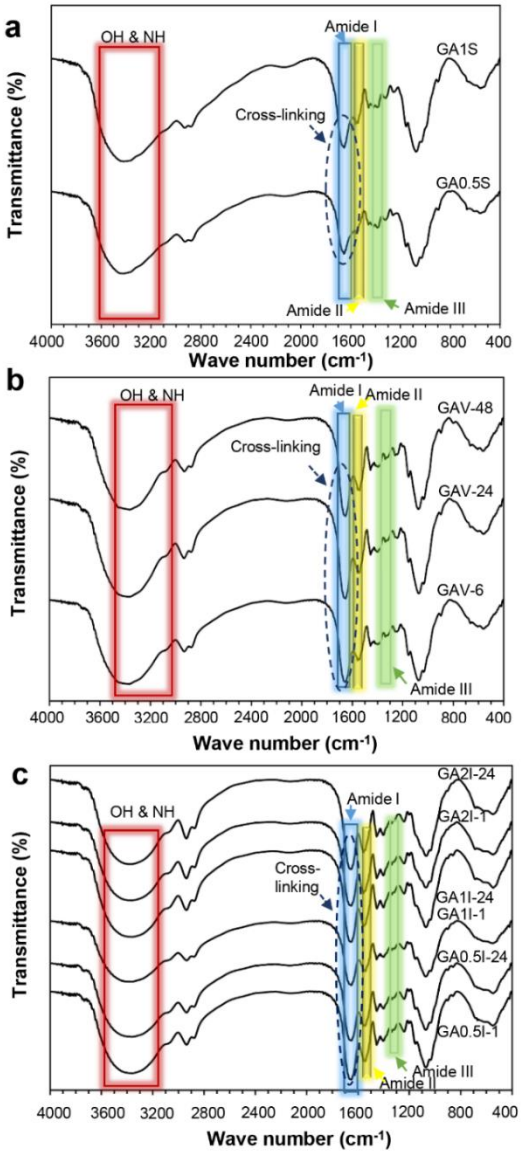


**Figure 3.** FTIR spectra of GA cross-linked gelatin/chitosan scaffolds with addition to (a) solution; (b) vapor exposure; and (c) immersion techniques

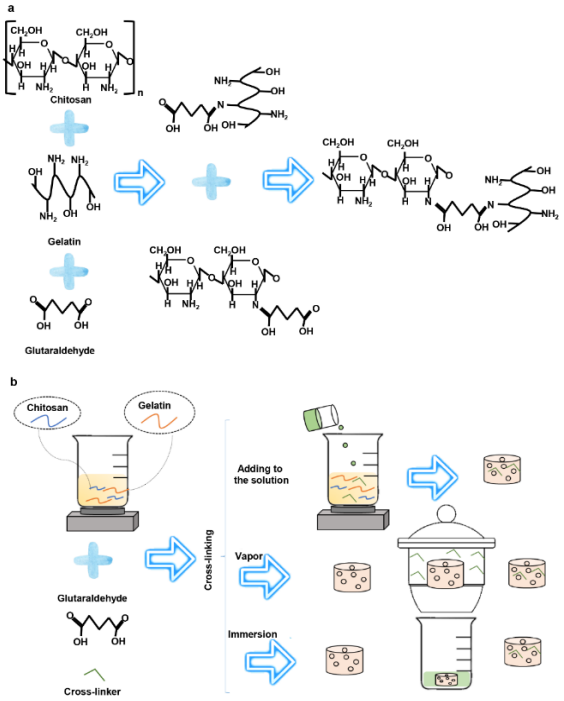


**Figure 4.** (a) Proposed schematic of the reaction between GA cross-linked gelatin and chitosan; (b) the schematic of scaffold preparation using different cross-linking methods

**3. 3. Water-Scaffolds Interactions** Herein, the swelling capability of all fabricated scaffolds was measured by soaking in PBS solution. The swelling ratio of GA cross-linked scaffolds with different methods of addition to the solution, vapor exposure, and immersion technique are demonstrated in Figure 5(a-c), respectively. As can be seen in Figure 5, GA cross-linking method affected the swelling ratio, besides GA concentration and time. In the solution addition method, the GA1S absorbed lower fluid than GA0.5S samples, and the swelling ratio was reduced from 35.55±3.1 to 22.31±1.3 (%) in 120 min PBS solution soaking. GAV-6, GAV-24, and GAV-48 scaffolds showed 33.12±0.21, 31.13±0.97, and 19.37±1.98 swelling capacity after 120 min immersion in PBS solution, respectively. In addition, after 120 min, swelling ratio was reached 26.59±3.97, 23.82±4.97, 26.23±0.13, 20.10±1.79, 22.49±2.89, and 16.55±0.57, for GA0.5I-1, GA0.5I-24, GA1I-1, GA1I-24, GA2I-1, and GA2I-24 scaffolds, respectively. Uncross-linked Gelatin/chitosan scaffold was considered as a control sample.

Swelling ratio is an essential factor in cell-scaffolds interactions, biodegradation ratio, and bioactivity in tissue engineering. A high swelling ratio leads to scaffolds' weight loss and structural deformation [34]. Gelatin is a hydrogel with a high capacity to absorb water and should be cross-linked before usage to regulating gelatin swelling capacity [55]. According to the achieved

results, the swelling ratio of each GA cross-linked sample was increased during 120 min. In general, GA cross-linking concentration and swelling time addition decreased the swelling ratio compared with control sample independence of crosslinking method. The higher GA concentration leads to the cross-linking bridge in the structure, especially with amine groups of chitosan. On the other hand, the higher cross-linked volume compacts the structure and limits chain movement [23]. In addition, high cross-likening duration increases the chance of cross-linker to react with the functional groups. Both cross-linked solution samples had lower swelling capacity compared with vapor cross-linked samples for 6 and 24 h. Whereas GA vapor cross-linked scaffolds for 48 h demonstrated lower swelling capacity. GA exposure duration influenced the swelling ratio in vapor cross-linked scaffolds. As the duration of cross-linking increased, the cross-linker had more opportunity to penetrate the structure and thus cross-linked the larger structure volume. Therefore, these achieved results were in line with a previous study by Kulkarni et al. [56], which showed that crosslinking exposure time led to a lower swelling ratio. The same trend was found in immersion samples and the 24 h immersed scaffolds had a lower than 1 h swelling ratio. In addition, the higher cross-link ratio reduced the swelling capacity. There was a slight irregularity in the decreasing trend of these samples, which can be attributed to the irregularity of the pores in the freezing process, which can be ignored. The more interesting result was that according to the results it seemed the cross-linking duration had more effect on swelling ratio than cross-linking concentration in immersion technique.

**3. 4. Biodegradation Ratio** In this study, scaffolds were immersed in PBS solution to evaluate biodegradability. The results are shown in Figure 5(d-f). Cross-inker free control sample demonstrated the most biodegradation ratio and had 51.16 ± 2.16 (%) biodegradation ratio after 2 weeks. GA1S, GAV-48, GAI-24 scaffolds with biodegradation ratio of 26.33±4.47, 22.53±4.44, and 21.72±72, respectively, demonstrated the lowest biodegradation ratio compared with other samples.

To allow new bone formation, bone tissue-engineered scaffolds must be biodegradable with a match biodegrading ratio with new bone tissue growth. Therefore, one of the critical parameters that are studied in bone tissue engineering is biodegradability [30]. The high biodegradation ratio in control sample was not unexpected as both chitosan and gelatin are hydrophilic and have a high degradation rate. Gelatin usually hydrolyzes in the presence of water quickly [57]. In GA cross-linked samples, the higher cross-linker concentration and exposure time decreased the biodegradation ratio. This phenomenon is consistent with the data previously published by Zhu et al. [34], where the higher exposure time to GA vapor cross-linker led to a lower biodegradation ratio. In general, the increasing cross-linker concentration reduced the biodegradation rate regardless of cross-linking method. In GA cross-linked samples, GA2I-24 indicated the lowest biodegradation and swelling ratio among all scaffolds. GA vapor cross-linked scaffolds showed the most biodegradation ratio even though they did not have the highest swelling ratio. This phenomenon may arise from low mechanical stability and insufficient penetration of the cross-linker into the inner layers of the structure. Because after the biodegradation of the initial layers, the bio-degradation process has been accelerated within two weeks. In general, the increasing cross-linker concentration reduced the biodegradation rate regardless of cross-linking method.

Due the presence of hydrophilic groups such as amide and carboxyl in gelatin structures, it hydrolyzed quickly in the presence of water. In addition, other studies indicated that *in-vivo* gelatin biodegradation was conducted by both hydrolysis and enzymatic manners [38, 58]. Besides, the PBS soaking of chitosan can lead to the 1,4 N-acetyl-glucosamine groups hydrolysis and created amino sugars. In the body environment, the degradation products can follow glycosaminoglycans and glycoprotein metabolic pathways or excreted from body [59]. GA cross-linking decreases biodegradation ratio by limitation of fluidic penetration and increasing the hydrophobicity. This low permeability of the aqueous solution delays the formation of smaller polymer residues, which are usually rapidly hydrolyzed in water. During the time, cross-link bonding breaks and facilities fluid penetration, which terminate to degradation of scaffolds [57, 60]. Here, the higher concentration and GA exposure time provided more favorable degradation ratio for bone replacement, while the other properties should be considered for introducing the best bone candidate.

**3. 5. Mechanical Strength** Here, the GA cross-linked scaffolds' mechanical properties were investigated, and the results are summarized in Figure 6. Figure 6(a) shows the compressive strength and (b) elastic modulus of the scaffolds. The lowest elastic modulus and compressive strength were achieved for the control group with 0.02 ± 0.15 MPa and 0.058±0.004 MPa, respectively. The compressive strength of the scaffolds were 0.06±0.013, 1.45±0.05, 0.08±0.01, 0.94±0.07, 1.12±0.18, 0.07±0.01, 1.03±0.08, 1.36±0.19, 1.87±0.22, 1.42±0.03, 2.24±0.09 MPa for GA0.5S, GA1S, GAV-6, GAV-24, GAV-48, GA0.5I-1, GA0.5I-24, GA1I-1, GA1I-24, GA2-1, GA2I-24, respectively and the elastic modulus was achieved 0.13±0.01, 3.87±1.01, 0.50±0.01, 1.03±0.54, 2.53±0.09, 0.45±0.046, 1.67±0.90, 2.88±0.04, 5.63±0.87, 3.75±0.07, 11.49±,0.41 MPa, respectively.

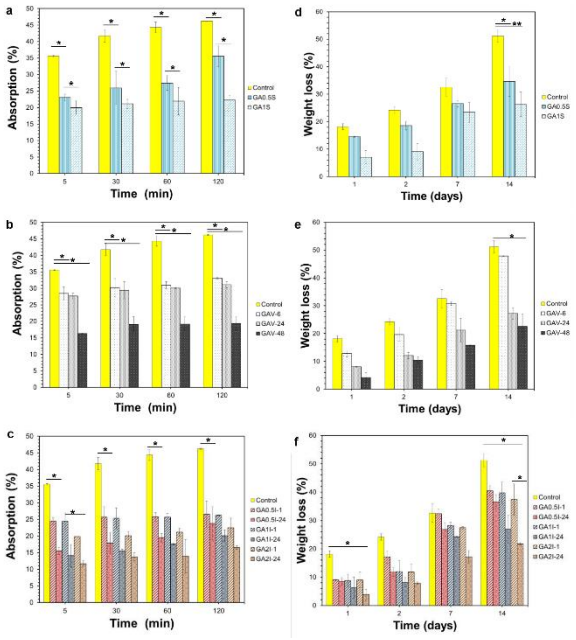


**Figure 5.** Swelling capacity of GA cross-linked gelatin/chitosan scaffolds with (a) addition to solution; (b) vapor exposure; and (c) immersion techniques during 120 min soaking in PBS solution. Weight loss of the GA cross-linked gelatin/chitosan scaffolds with (d) addition to solution; (e) vapor exposure; and (f) immersion techniques during 2 week immersion in PBS solution

The mechanical properties measurements of the fabricated scaffolds were necessary to estimate the scaffolds' load-bearing capacity in the bone defects [61]. The material type, cross-linker degree, and pore size influenced the compressive moduli of the scaffold [62]. The cross-linking of the composition increased the modulus and compressive strength compared to the control sample. In GA1S scaffolds, the elastic modulus and compressive strength was higher than GA0.5S. These results were in line with previous reports, introducing the cross-linker concentration as one of the influential factors on the stronger mechanical properties [53]. In addition in another study, Putri et al. [63] demonstrated the addition of GA with the concentration of 5 vol% relative to the total mixture to the chitosan and gelatin solution increased the compressive strength to 3.3 ± 0.3 MPa in comparison with non-cross-linked sample with 1.7 ± 0.2 MPa, compressive strength; whereas the relative higher compressive modulus in their study can be related to the β-tricalcium phosphate addition to the gelatin and chitosan composites. On the other hand, in the GA vapor cross-linking method, 48 h exposing increased the elastic modulus. According to the achieved data in the immersion technique, the more GA concentration and cross-linker soaking time increased the elastic module of the scaffolds. It seems the cross-linking exposure time had more effect than concentration. According to the compressive strength of natural trabecular and cortical bone (0.1–16 MPa and 130–200 MPa [64]), the scaffolds with higher compressive strength were more favorable for bone regeneration. Therefore, GA1S, GAV-48, GA1I-1, GA1I-24, GA2I-1, GA2I-24 scaffolds with higher compressive strength and elastic modulus were chosen for further investigations.

**3. 6. Contact Angle** Water-drop contact angle of the GA1S, GAV-48, GA1I-1, GA1I-24, GA2I-1, GA2I-24 scaffolds was measured as an indicator of hydrophilic/hydrophobic behavior. The results are demonstrated in Figure 7. Water contact angle of control, GA1S, GAV-48, GA1I-1, GA1I-24, GA2I-1, GA2I-24 was measured as 39.3°, 58.3°, 76.9°, 42.2°, 76.7°, 59.0°, and 106.4°, respectively.

More hydrophilic surfaces demonstrate lower contact angle and show enhanced cell adhesion and proliferation [65]. Although chitosan and gelatin have hydrophilic functional groups, blending the chitosan with gelatin reduces hydrophilicity [66]. This effect can be related to the interaction between the functional groups of gelatin and chitosan with different charge side chains and neutralize charge complex formation with reduced charge density and polarity. The non-cross-linked scaffolds demonstrated the lowest contact angle. This can be related to the lower compact volume and free

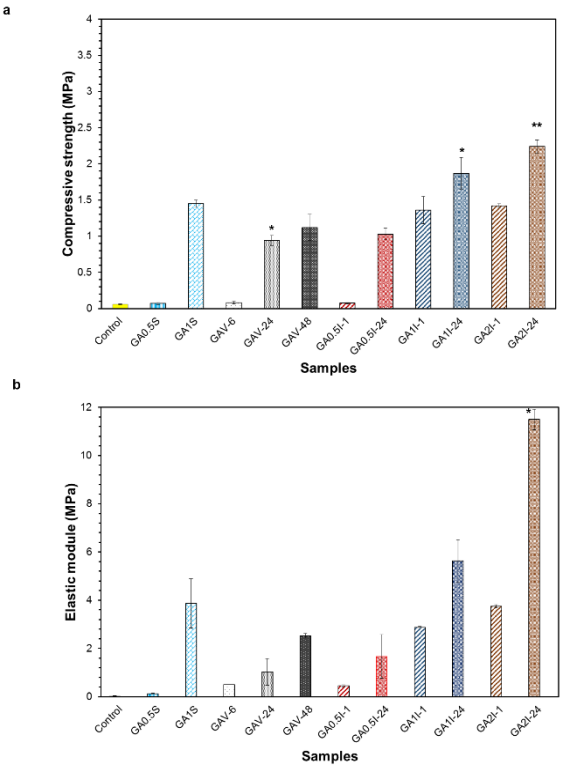


**Figure 6.** (a) The compressive strength and (b) elastic modulus of all samples

hydrophilic functional groups of chitosan and gelatin. In general, the scaffolds' contact angle was reduced by adding cross-linker concentration and exposing time in GA cross-linked sample. It was expected according to the results of swelling ratio and biodegradation properties. The high swelling and biodegradation property of the chitosan/gelatin scaffolds can be attributed to the gelatin dissolution in watery fluids and opening the interacted functional groups of chitosan and gelatin followed by interaction with $H_2O$ molecules during the soaking time in addition to the lower compact and non-cross-linked volume. It should be noted that the scaffolds with a contact angle in the range of approximately 20-70 ° are more favorable for cell interactions [67, 68]. Therefore, it is expected GA1S, GA1I-1, and GA2I-1 demonstrate the best cell behavior. Among these three samples and according to the achieved physicochemical results, GA1S sample was selected as the optimum sample and introduced for more cellular investigations.

**3. 7. Cell-Scaffold Behavior** This study performed cell studies on the optimum sample (GA1S) based on the above results to evaluate the BMSCs morphology, proliferation, and cell differentiation. As shown in Figure 8(a), cells were well attached to the surface of the sample. Also, cells were created filopodia and well spread all over the scaffold. According to the MTT results (Figure 8(b)), the GA1S showed lower cell viability than the control sample in 2 and 4 days, but after 7 days GA1S scaffold showed accelerated cell proliferation and demonstrated higher cell viability compared with the control sample. According to ALP relative expression results of GA1S sample (Figure 8(c)), ALP level was approximately equal with control specimen, while after 7 days, there was an increase in ALP expression compared with the control scaffold. After 14 days, the ALP expression was accelerated and significantly higher than the control scaffold. To further investigate the bone differentiation of cultured cells, OC and RUNX2 expression was measured in GA1S scaffold, and the results are shown in Figure 8 (d and e), respectively. There was a similar trend in OC expression, and there was a significantly higher expression in GA1S sample compared with the control. A relatively lower RUNX2 expression was detected in GA1S scaffold in 7th and 14th days of incubation.

The well cell adhesion and filopodia formation on GA1S scaffold can be due to the biocompatibility nature of both polymers, and on the other hand, the glycine, proline, and hydroxyproline residues of gelatin [69, 70]. The relatively lower cell viability in first days may be related to absorbed GA on the surface. According to Figure 8 (b, insert), it should be

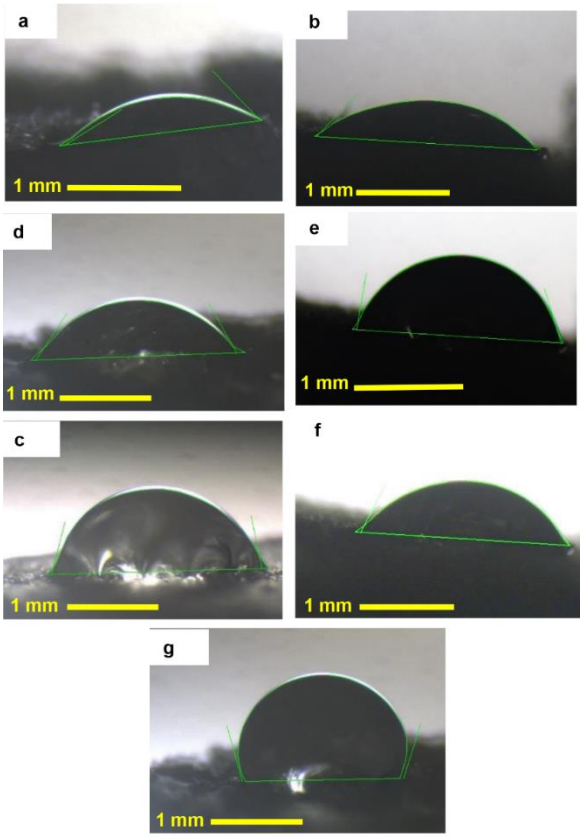


**Figure 7.** The contact angle of the (a) control; (b) GA1S; (c) GAV-48; (d) GA1I-1; (e) GA1I-24; (f) GA2I-1; and (g) GA2I-24 gelatin/chitosan scaffolds

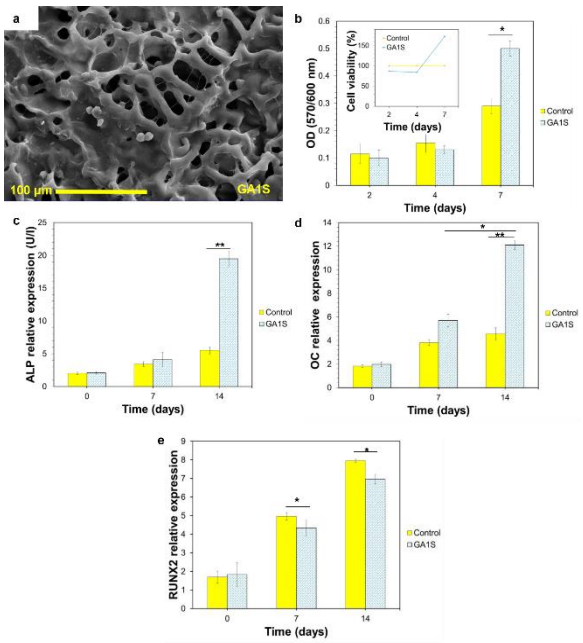


**Figure 8.** (a) FESEM micrograph of cell cultured morphology on the surface of GA1S scaffold; (b) the results of cell viability during 7 days of cell culturing. (c) ALP; (d) OC; and (e) RUNX2 expression level during 14 days of cell incubation on the surface of GA1S scaffold

noted that although the GA1S sample showed a slight decrease in cell viability compared to the control sample in the early days, it was in the acceptable range and had more than 80% cell viability on all days.

ALP is an osteoblastic activity and mineralization indicator, an initial osteoblastic differentiation marker [71]. The ALP expression was increased during 14 days and showed higher values in compare to the control sample. OC and RUNX2 are essential genes of osteoblastic differentiation [72]. RUNX2 is a middle and OC is a late-stage marker of osteogenic differentiation [73]. OC as a noncollagenous protein in bone ECM increases bone formation and has a high affinity for calcium ions in mineralization and apatite deposition [74]. Therefore, high expression of OC in GA1S scaffold could help mineralization and bone formation. However, a relatively lower RUNX2 expression was detected in GA1S scaffold in 7th and 14th days of incubation, while the RUNX2 expression proved the osteoblastic differentiation.

## 4. CONCLUSIONS

Cross-linking concentration, exposure time, and applied technique had a lot of effect on the properties of GA cross-linked gelatin/chitosan scaffolds. In general, according to the morphological observation, the obtained freeze-dried structure was porous with open porosity in all the used techniques. The average pore sizes were in the suitable range for bone tissue engineering. The samples cross-linked by GA vapor exposure had a more uniform structure than samples cross-linked with other methods. On the other hand, it was demonstrated that the higher GA cross-linker or higher exposure time intensified C=N related peak and confirmed the higher cross-linking percentage. Also, the higher GA cross-linking exposing duration and concentration decreased swelling ratio and biodegradation ratio while improved the mechanical properties. It was revealed that the cross-linking exposure time had more effect than concentration on mechanical properties and only higher GA concentration or longer GA exposure time showed an acceptable mechanical properties for bone regeneration. Contact angle results of the candidate samples confirmed the swelling results and the contact angle was reduced by cross-linker concentration and exposure time increasing and GA1S sample demonstrated a 39.3° contact angle. The cellular studies was performed on the selected specimen (GA1S) for further investigations. Cell adhesion, and viability results demonstrated the high cell supporting behavior of GA1S scaffolds. In addition, the GA1S scaffold led to the osteo-related genes expression such as ALP, OC, and RUNX2. As the result of all experiments, the GA1S sample was introduced as the optimum scaffold, and it can be useful for bone tissue engineering applications.

**Author Contributions:** Ideas and evolution of overarching goals, development and creation of models, conducting an investigation process, and preparation of the manuscript were done by FB. DL cooperate in in-vitro data collection and analysis procedures. Leadership responsibility for the activity planning and execution, including mentorship external to the core team and acquisition of the financial support for the project leading to this publication, were performed by CY and AZ.

**Funding:** This work was supported by the Scientific Research Foundation provided by Pudong Hospital affiliated to Fudan University (Project no. YJRCJJ201906), the Talents Training Program of Pudong Hospital affiliated to Fudan University (Project no. PX202001), the Youth Science and Technology Project of Health Commission of Shanghai Pudong New Area (Project no. PW2020B-5), the Outstanding Clinical Discipline Project of Shanghai Pudong (Grant No. PWYgy2018-09).

**Data Availability Statement:** The datasets generated for this study are available on request to the corresponding author

**Acknowledgments:** Special thanks must go to Dr. Farnaz Ghorbani from the institute of Biomaterials, University of Erlangen-Nuremberg. Her expert knowledge in the field of tissue engineering scaffolds is a worthy addition to this text.

**Conflicts of Interest:** The authors whose names are listed certify that they have NO affiliations with or involvement in any organization or entity with any financial interest, or non-financial interest in the subject matter or materials discussed in this manuscript.

## 5. REFERENCES

1. Koons, G.L., Diba, M. and Mikos, A.G., "Materials design for bone-tissue engineering", ***Nature Reviews Materials***, Vol. 5, No. 8, (2020), 584-603. https://doi.org/10.1038/s41578-020-0204-2
2. Guillaume, O., Geven, M., Sprecher, C., Stadelmann, V., Grijpma, D., Tang, T., Qin, L., Lai, Y., Alini, M. and De Bruijn, J., "Surface-enrichment with hydroxyapatite nanoparticles in stereolithography-fabricated composite polymer scaffolds promotes bone repair", ***Acta Biomaterialia***, Vol. 54, (2017), 386-398. https://doi.org/10.1016/j.actbio.2017.03.006
3. Pereira, H.F., Cengiz, I.F., Silva, F.S., Reis, R.L. and Oliveira, J.M., "Scaffolds and coatings for bone regeneration", ***Journal of Materials Science: Materials in Medicine***, Vol. 31, No. 3, (2020), 1-16.
4. Hassanzadeh Nemati, N. and Mirhadi, S.M., "Synthesis and characterization of highly porous $TiO_2$ scaffolds for bone defects", ***International Journal of Engineering, Transactions A: Basics***, , Vol. 33, No. 1, (2020), 134-140. https://doi.org/10.5829/ije.2020.33.01a.15
5. Liu, D., Nie, W., Li, D., Wang, W., Zheng, L., Zhang, J., Zhang, J., Peng, C., Mo, X. and He, C., "3d printed pcl/srha scaffold for enhanced bone regeneration", ***Chemical Engineering Journal***, Vol. 362, (2019), 269-279. https://doi.org/10.1016/j.cej.2019.01.015

6. Sadeghinia, A., Soltani, S., Aghazadeh, M., Khalilifard, J. and Davaran, S., "Design and fabrication of clinoptilolite–nanohydroxyapatite/chitosan–gelatin composite scaffold and evaluation of its effects on bone tissue engineering", ***Journal of Biomedical Materials Research Part A***, Vol. 108, No. 2, (2020), 221-233. https://doi.org/10.1002/jbm.a.36806
7. Sultana, N., Hassan, M., Ridzuan, N., Ibrahim, Z. and Soon, C., "Fabrication of gelatin scaffolds using thermally induced phase separation technique", ***International Journal of Engineering***, Vol. 31, No. 8, (2018), 1302-1307. https://doi.org/10.5829/ije.2018.31.08b.19
8. Raja, N. and Yun, H.-s., "A simultaneous 3d printing process for the fabrication of bioceramic and cell-laden hydrogel core/shell scaffolds with potential application in bone tissue regeneration", ***Journal of Materials Chemistry B***, Vol. 4, No. 27, (2016), 4707-4716. https://doi.org/10.1039/C6TB00849F
9. Sarparast, Z., Abdoli, R., Rahbari, A., Varmazyar, M. and Reza Kashyzadeh, K., "Experimental and numerical analysis of permeability in porous media", ***International Journal of Engineering***, ***Transactions B: Applications,*** Vol. 33, No. 11, (2020), 2408-2415. https://doi.org/10.5829/ije.2020.33.11b.31
10. Ilyas, R. and Sapuan, S., "The preparation methods and processing of natural fibre bio-polymer composites", ***Current Organic Synthesis***, Vol. 16, No. 8, (2019), 1068-1070. https://doi.org/10.2174/1570179416082001201056l6
11. Ilyas, R., Sapuan, S., Harussani, M., Hakimi, M., Haziq, M., Atikah, M., Asyraf, M., Ishak, M., Razman, M. and Nurazzi, N., "Polylactic acid (PLA) biocomposite: Processing, additive manufacturing and advanced applications", ***Polymers***, Vol. 13, No. 8, (2021), 1326. https://doi.org/10.3390/polym13081326
12. Ilyas, R.A., Sapuan, S.M., Ibrahim, R., Abral, H., Ishak, M., Zainudin, E., Asrofi, M., Atikah, M.S.N., Huzaifah, M.R.M. and Radzi, A.M., "Sugar palm (arenga pinnata (wurmb.) merr) cellulosic fibre hierarchy: A comprehensive approach from macro to nano scale", ***Journal of Materials Research and Technology***, Vol. 8, No. 3, (2019), 2753-2766. https://doi.org/10.1016/j.jmrt.2019.04.011
13. Ilyas, R., Sapuan, S., Ishak, M. and Zainudin, E., "Sugar palm nanofibrillated cellulose (arenga pinnata (wurmb.) merr): Effect of cycles on their yield, physic-chemical, morphological and thermal behavior", ***International Journal of Biological Macromolecules***, Vol. 123, No., (2019), 379-388. https://doi.org/10.1016/j.ijbiomac.2018.11.124
14. Ilyas, R., Zuhri, M., Aisyah, H., Asyraf, M., Hassan, S., Zainudin, E., Sapuan, S., Sharma, S., Bangar, S. and Jumaidin, R., "Natural fiber-reinforced polylactic acid, polylactic acid blends and their composites for advanced applications", ***Polymers***, Vol. 14, No. 1, (2022), 202. https://doi.org/10.3390/polym14010202
15. Ilyas, R., Zuhri, M., Norrrahim, M.N.F., Misenan, M.S.M., Jenol, M.A., Samsudin, S.A., Nurazzi, N., Asyraf, M., Supian, A. and Bangar, S.P., "Natural fiber-reinforced polycaprolactone green and hybrid biocomposites for various advanced applications", ***Polymers***, Vol. 14, No. 1, (2022), 182. https://doi.org/10.3390/polym14010182
16. Tang, G., Tan, Z., Zeng, W., Wang, X., Shi, C., Liu, Y., He, H., Chen, R. and Ye, X., "Recent advances of chitosan-based injectable hydrogels for bone and dental tissue regeneration", ***Frontiers in Bioengineering and Biotechnology***, Vol. 8, (2020), 587658. https://doi.org/10.3389/fbioe.2020.587658
17. Prakash, J., Prema, D., Venkataprasanna, K., Balagangadharan, K., Selvamurugan, N. and Venkatasubbu, G.D., "Nanocomposite chitosan film containing graphene oxide/hydroxyapatite/gold for bone tissue engineering", ***International Journal of Biological Macromolecules***, Vol. 154, (2020), 62-71. https://doi.org/10.1016/j.ijbiomac.2020.03.095
18. Vaidhyanathan, B., Vincent, P., Vadivel, S., Karuppiah, P., AL-Dhabi, N.A., Sadhasivam, D.R., Vimalraj, S. and Saravanan, S., "Fabrication and investigation of the suitability of chitosan-silver composite scaffolds for bone tissue engineering applications", ***Process Biochemistry***, Vol. 100, (2021), 178-187. https://doi.org/10.1016/j.procbio.2020.10.008
19. De Witte, T.M., Wagner, A.M., Fratila-Apachitei, L.E., Zadpoor, A.A. and Peppas, N.A., "Immobilization of nanocarriers within a porous chitosan scaffold for the sustained delivery of growth factors in bone tissue engineering applications", ***Journal of Biomedical Materials Research Part A***, Vol. 108, No. 5, (2020), 1122-1135. https://doi.org/10.1002/jbm.a.36887
20. Badawy, M.E., Taktak, N.E., Awad, O.M., Elfiki, S.A. and El-Ela, N.E.A., "Preparation and characterization of biopolymers chitosan/alginate/gelatin gel spheres crosslinked by glutaraldehyde", ***Journal of Macromolecular Science, Part B***, Vol. 56, No. 6, (2017), 359-372. https://doi.org/10.1080/00222348.2017.1316640
21. Sharma, S., Sudhakara, P., Singh, J., Ilyas, R., Asyraf, M. and Razman, M., "Critical review of biodegradable and bioactive polymer composites for bone tissue engineering and drug delivery applications", ***Polymers***, Vol. 13, No. 16, (2021), 2623. https://doi.org/10.3390/polym13162623
22. Choi, Y.-J., Park, H., Ha, D.-H., Yun, H.-S., Yi, H.-G. and Lee, H., "3d bioprinting of in vitro models using hydrogel-based bioinks", ***Polymers***, Vol. 13, No. 3, (2021), 366. https://doi.org/10.3390/polym13030366
23. Zarif, M.-E., "A review of chitosan-, alginate-, and gelatin-based biocomposites for bone tissue engineering", ***Biomater. Tissue Eng. Bull***, Vol. 5, (2018), 97-109.
24. Oryan, A., Kamali, A., Moshiri, A., Baharvand, H. and Daemi, H., "Chemical crosslinking of biopolymeric scaffolds: Current knowledge and future directions of crosslinked engineered bone scaffolds", ***International Journal of Biological Macromolecules***, Vol. 107, (2018), 678-688. https://doi.org/10.1016/j.ijbiomac.2017.08.184
25. Ehrmann, A., "Non-toxic crosslinking of electrospun gelatin nanofibers for tissue engineering and biomedicine—a review", ***Polymers***, Vol. 13, No. 12, (2021), 1973. https://doi.org/10.3390/polym13121973
26. Lee, J.B., Ko, Y.-G., Cho, D., Park, W.H. and Kwon, O.H., "Modification and optimization of electrospun gelatin sheets by electron beam irradiation for soft tissue engineering", ***Biomaterials Research***, Vol. 21, No. 1, (2017), 1-9. https://doi.org/10.1186/s40824-017-0100-z
27. Campiglio, C.E., Contessi Negrini, N., Farè, S. and Draghi, L., "Cross-linking strategies for electrospun gelatin scaffolds", ***Materials***, Vol. 12, No. 15, (2019), 2476. https://doi.org/10.3390/ma12152476
28. Yang, G., Xiao, Z., Long, H., Ma, K., Zhang, J., Ren, X. and Zhang, J., "Assessment of the characteristics and biocompatibility of gelatin sponge scaffolds prepared by various crosslinking methods", ***Scientific Reports***, Vol. 8, No. 1, (2018), 1-13. https://doi.org/10.1038/s41598-018-20006-y
29. Pauly, M.P., Tucker, L.-Y., Szpakowski, J.-L., Ready, J.B., Baer, D., Hwang, J. and Lok, A.S.-F., "Incidence of hepatitis b virus reactivation and hepatotoxicity in patients receiving long-term treatment with tumor necrosis factor antagonists", ***Clinical Gastroenterology and Hepatology***, Vol. 16, No. 12, (2018), 1964-1973. e1961. https://doi.org/10.1016/j.cgh.2018.04.033
30. Liu, Y., Ma, L. and Gao, C., "Facile fabrication of the glutaraldehyde cross-linked collagen/chitosan porous scaffold for skin tissue engineering", ***Materials Science and Engineering: c***, Vol. 32, No. 8, (2012), 2361-2366. https://doi.org/10.1016/j.msec.2012.07.008

31. Nguyen, T.-H. and Lee, B.-T., "Fabrication and characterization of cross-linked gelatin electro-spun nano-fibers", ***Journal of Biomedical Science and Engineering***, Vol. 3, No. 12, (2010), 1117. https://doi.org/10.4236/jbise.2010.312145
32. Destaye, A.G., Lin, C.-K. and Lee, C.-K., "Glutaraldehyde vapor cross-linked nanofibrous pva mat with in situ formed silver nanoparticles", ***ACS Applied Materials & Interfaces***, Vol. 5, No. 11, (2013), 4745-4752. https://doi.org/10.1021/am401730x
33. Yang, Y., Ritchie, A.C. and Everitt, N.M., "Comparison of glutaraldehyde and procyanidin cross-linked scaffolds for soft tissue engineering", ***Materials Science and Engineering: c***, Vol. 80, (2017), 263-273. https://doi.org/10.1016/j.msec.2017.05.141
34. Zhu, B., Li, W., Chi, N., Lewis, R.V., Osamor, J. and Wang, R., "Optimization of glutaraldehyde vapor treatment for electrospun collagen/silk tissue engineering scaffolds", ***ACS Omega***, Vol. 2, No. 6, (2017), 2439-2450. https://doi.org/10.1021/acsomega.7b00290
35. Kaczmarek, B., Sionkowska, A., Monteiro, F., Carvalho, A., Łukowicz, K. and Osyczka, A., "Characterization of gelatin and chitosan scaffolds cross-linked by addition of dialdehyde starch", ***Biomedical Materials***, Vol. 13, No. 1, (2017), 015016. https://doi.org/10.1088/1748-605X/aa8910
36. Maji, K., Dasgupta, S., Pramanik, K. and Bissoyi, A., "Preparation and evaluation of gelatin-chitosan-nanobioglass 3d porous scaffold for bone tissue engineering", ***International Journal of Biomaterials***, Vol. 2016, (2016). https://doi.org/10.1155/2016/9825659
37. Nokoorani, Y.D. and Shamloo, A., "Comparison of the effect of edc and glutaraldehyde as cross-linkers on morphology and swelling ratio of gelatin/chitosan scaffolds for use in skin tissue engineering", in 2018 25th National and 3rd International Iranian Conference on Biomedical Engineering (ICBME), IEEE. (2018), 1-4.
38. Rezaei, H., Asefnejad, A., Joupari, M.D. and Joughehdoust, S., "The physicochemical and mechanical investigation of siloxane modified gelatin/sodium alginate injectable hydrogels loaded by ascorbic acid and β-glycerophosphate", ***Materials Today Communications***, Vol. 26, (2021), 101914. https://doi.org/10.1016/j.mtcomm.2020.101914
39. Ghorbani, F., Zamanian, A. and Sahranavard, M., "Mussel-inspired polydopamine-mediated surface modification of freeze-cast poly (ε-caprolactone) scaffolds for bone tissue engineering applications", ***Biomedical Engineering/Biomedizinische Technik***, Vol. 65, No. 3, (2020), 273-287. https://doi.org/10.1515/bmt-2019-0061
40. Ghorbani, F., Sahranavard, M. and Zamanian, A., "Immobilization of gelatin on the oxygen plasma-modified surface of polycaprolactone scaffolds with tunable pore structure for skin tissue engineering", ***Journal of Polymer Research***, Vol. 27, No. 9, (2020), 1-12. https://doi.org/10.1007/s10965-020-02263-6
41. Hassanzadeh Nemati, N., Ghasempour, E. and Zamanian, A., "Effect of dual releasing of β-glycerophosphate and dexamethasone from ti nanostructured surface for using in orthopedic applications", ***International Journal of Engineering, Transactions A: Basics,***, Vol. 32, No. 10, (2019), 1337-1344. https://doi.org/10.5829/ije.2019.32.10a.01
42. Ghorbani, F., Ghalandari, B., Sahranavard, M., Zamanian, A. and Collins, M.N., "Tuning the biomimetic behavior of hybrid scaffolds for bone tissue engineering through surface modifications and drug immobilization", ***Materials Science and Engineering: c***, Vol. 130, (2021), 112434. https://doi.org/10.1016/j.msec.2021.112434
43. Ghorbani, F., Zamanian, A., Behnamghader, A. and Joupari, M.D., "Microwave-induced rapid formation of biomimetic hydroxyapatite coating on gelatin-siloxane hybrid microspheres in 10x-sbf solution", ***e-Polymers***, Vol. 18, No. 3, (2018), 247-255. https://doi.org/10.1515/epoly-2017-0196
44. Ghafari, R., Jonoobi, M., Amirabad, L.M., Oksman, K. and Taheri, A.R., "Fabrication and characterization of novel bilayer scaffold from nanocellulose based aerogel for skin tissue engineering applications", ***International Journal of Biological Macromolecules***, Vol. 136, (2019), 796-803. https://doi.org/10.1016/j.ijbiomac.2019.06.104
45. Thein-Han, W., Saikhun, J., Pholpramoo, C., Misra, R. and Kitiyanant, Y., "Chitosan–gelatin scaffolds for tissue engineering: Physico-chemical properties and biological response of buffalo embryonic stem cells and transfectant of gfp–buffalo embryonic stem cells", ***Acta Biomaterialia***, Vol. 5, No. 9, (2009), 3453-3466. https://doi.org/10.1016/j.actbio.2009.05.012
46. Lee, J.H., Park, T.G., Park, H.S., Lee, D.S., Lee, Y.K., Yoon, S.C. and Nam, J.-D., "Thermal and mechanical characteristics of poly (l-lactic acid) nanocomposite scaffold", ***Biomaterials***, Vol. 24, No. 16, (2003), 2773-2778. https://doi.org/10.1016/S0142-9612(03)00080-2
47. Sattary, M., Rafienia, M., Khorasani, M.T. and Salehi, H., "The effect of collector type on the physical, chemical, and biological properties of polycaprolactone/gelatin/nano-hydroxyapatite electrospun scaffold", ***Journal of Biomedical Materials Research Part B: Applied Biomaterials***, Vol. 107, No. 4, (2019), 933-950. https://doi.org/10.1002/jbm.b.34188
48. Abbasi, N., Hamlet, S., Love, R.M. and Nguyen, N.-T., "Porous scaffolds for bone regeneration", ***Journal of Science: Advanced Materials and Devices***, Vol. 5, No. 1, (2020), 1-9. https://doi.org/10.1016/j.jsamd.2020.01.007
49. Chen, H., Xing, X., Tan, H., Jia, Y., Zhou, T., Chen, Y., Ling, Z. and Hu, X., "Covalently antibacterial alginate-chitosan hydrogel dressing integrated gelatin microspheres containing tetracycline hydrochloride for wound healing", ***Materials Science and Engineering: c***, Vol. 70, (2017), 287-295. https://doi.org/10.1016/j.msec.2016.08.086
50. Ding, Y., Yin, H., Shen, S., Sun, K. and Liu, F., "Chitosan-based magnetic/fluorescent nanocomposites for cell labelling and controlled drug release", ***New Journal of Chemistry***, Vol. 41, No. 4, (2017), 1736-1743. https://doi.org/10.1039/C6NJ02897G
51. Baniasadi, H., SA, A.R. and Mashayekhan, S., "Fabrication and characterization of conductive chitosan/gelatin-based scaffolds for nerve tissue engineering", ***International Journal of Biological Macromolecules***, Vol. 74, (2015), 360-366. https://doi.org/10.1016/j.ijbiomac.2014.12.014
52. Sharma, C., Dinda, A.K., Potdar, P.D., Chou, C.-F. and Mishra, N.C., "Fabrication and characterization of novel nano-biocomposite scaffold of chitosan–gelatin–alginate–hydroxyapatite for bone tissue engineering", ***Materials Science and Engineering: c***, Vol. 64, (2016), 416-427. https://doi.org/10.1016/j.msec.2016.03.060
53. Hospodiuk, M., Dey, M., Sosnoski, D. and Ozbolat, I.T., "The bioink: A comprehensive review on bioprintable materials", ***Biotechnology Advances***, Vol. 35, No. 2, (2017), 217-239. https://doi.org/10.1016/j.biotechadv.2016.12.006
54. Patel, S., Srivastava, S., Singh, M.R. and Singh, D., "Preparation and optimization of chitosan-gelatin films for sustained delivery of lupeol for wound healing", ***International Journal of Biological Macromolecules***, Vol. 107, (2018), 1888-1897. https://doi.org/10.1016/j.ijbiomac.2017.10.056
55. Luo, Y., Li, Y., Qin, X. and Wa, Q., "3d printing of concentrated alginate/gelatin scaffolds with homogeneous nano apatite coating for bone tissue engineering", ***Materials & Design***, Vol. 146, (2018), 12-19. https://doi.org/10.1016/j.matdes.2018.03.002
56. Kulkarni, A.R., Soppimath, K.S., Aminabhavi, T.M., Dave, A.M. and Mehta, M.H., "Glutaraldehyde crosslinked sodium alginate beads containing liquid pesticide for soil application", ***Journal of***

***Controlled Release***, Vol. 63, No. 1-2, (2000), 97-105. https://doi.org/10.1016/S0168-3659(99)00176-5

57. Alizadeh, M., Abbasi, F., Khoshfetrat, A. and Ghaleh, H., "Microstructure and characteristic properties of gelatin/chitosan scaffold prepared by a combined freeze-drying/leaching method", ***Materials Science and Engineering: c***, Vol. 33, No. 7, (2013), 3958-3967. https://doi.org/10.1016/j.msec.2013.05.039
58. Bacakova, L., Zikmundova, M., Pajorova, J., Broz, A., Filova, E., Blanquer, A., Matejka, R., Stepanovska, J., Mikes, P. and Jencova, V., "Nanofibrous scaffolds for skin tissue engineering and wound healing based on synthetic polymers", ***Applications of Nanobiotechnology***, (2019), 1. https://doi.org/10.5772/intechopen.88744
59. Iqbal, H., Ali, M., Zeeshan, R., Mutahir, Z., Iqbal, F., Nawaz, M.A.H., Shahzadi, L., Chaudhry, A.A., Yar, M. and Luan, S., "Chitosan/hydroxyapatite (ha)/hydroxypropylmethyl cellulose (hpmc) spongy scaffolds-synthesis and evaluation as potential alveolar bone substitutes", ***Colloids and Surfaces B: Biointerfaces***, Vol. 160, (2017), 553-563. https://doi.org/10.1016/j.colsurfb.2017.09.059
60. Kavya, K., Dixit, R., Jayakumar, R., Nair, S.V. and Chennazhi, K.P., "Synthesis and characterization of chitosan/chondroitin sulfate/nano-sio2 composite scaffold for bone tissue engineering", ***Journal of Biomedical Nanotechnology***, Vol. 8, No. 1, (2012), 149-160. https://doi.org/10.1166/jbn.2012.1363
61. Kouhi, M., Morshed, M., Varshosaz, J. and Fathi, M.H., "Poly (ε-caprolactone) incorporated bioactive glass nanoparticles and simvastatin nanocomposite nanofibers: Preparation, characterization and in vitro drug release for bone regeneration applications", ***Chemical Engineering Journal***, Vol. 228, (2013), 1057-1065. https://doi.org/10.1016/j.cej.2013.05.091
62. Ji, C., Annabi, N., Khademhosseini, A. and Dehghani, F., "Fabrication of porous chitosan scaffolds for soft tissue engineering using dense gas co2", ***Acta Biomaterialia***, Vol. 7, No. 4, (2011), 1653-1664. https://doi.org/10.1016/j.actbio.2010.11.043
63. Putri, T.S., Rianti, D., Rachmadi, P. and Yuliati, A., "Effect of glutaraldehyde on the characteristics of chitosan–gelatin–β-tricalcium phosphate composite scaffolds", ***Materials Letters***, Vol. 304, (2021), 130672. https://doi.org/10.1016/j.matlet.2021.130672
64. Gerhardt, L.-C. and Boccaccini, A.R., "Bioactive glass and glass-ceramic scaffolds for bone tissue engineering", ***Materials***, Vol. 3, No. 7, (2010), 3867-3910. https://doi.org/10.3390/ma3073867
65. Nalvuran, H., Elçin, A.E. and Elçin, Y.M., "Nanofibrous silk fibroin/reduced graphene oxide scaffolds for tissue engineering and cell culture applications", ***International Journal of Biological Macromolecules***, Vol. 114, (2018), 77-84. https://doi.org/10.1016/j.ijbiomac.2018.03.072
66. Zhang, Z., Cheng, X., Yao, Y., Luo, J., Tang, Q., Wu, H., Lin, S., Han, C., Wei, Q. and Chen, L., "Electrophoretic deposition of chitosan/gelatin coatings with controlled porous surface topography to enhance initial osteoblast adhesive responses", ***Journal of Materials Chemistry B***, Vol. 4, No. 47, (2016), 7584-7595. https://doi.org/10.1039/c6tb02122k
67. Huang, Y., Hao, M., Nian, X., Qiao, H., Zhang, X., Zhang, X., Song, G., Guo, J., Pang, X. and Zhang, H., "Strontium and copper co-substituted hydroxyapatite-based coatings with improved antibacterial activity and cytocompatibility fabricated by electrodeposition", ***Ceramics International***, Vol. 42, No. 10, (2016), 11876-11888. https://doi.org/10.1016/j.ceramint.2016.04.110
68. Schnell, G., Staehlke, S., Duenow, U., Nebe, J.B. and Seitz, H., "Femtosecond laser nano/micro textured ti6al4v surfaces—effect on wetting and mg-63 cell adhesion", ***Materials***, Vol. 12, No. 13, (2019), 2210. https://doi.org/10.3390/ma12132210
69. Mahnama, H., Dadbin, S., Frounchi, M. and Rajabi, S., "Preparation of biodegradable gelatin/pva porous scaffolds for skin regeneration", ***Artificial Cells, Nanomedicine, and Biotechnology***, Vol. 45, No. 5, (2017), 928-935. https://doi.org/10.1080/21691401.2016.1193025
70. Liu, C., Kou, Y., Zhang, X., Dong, W., Cheng, H. and Mao, S., "Enhanced oral insulin delivery via surface hydrophilic modification of chitosan copolymer based self-assembly polyelectrolyte nanocomplex", ***International Journal of Pharmaceutics***, Vol. 554, (2019), 36-47. https://doi.org/10.1016/j.ijpharm.2018.10.068
71. Trivedi, S., Srivastava, K., Gupta, A., Saluja, T.S., Kumar, S., Mehrotra, D. and Singh, S.K., "A quantitative method to determine osteogenic differentiation aptness of scaffold", ***Journal of Oral Biology and Craniofacial Research***, Vol. 10, No. 2, (2020), 158-160. https://doi.org/10.1016/j.jobcr.2020.04.006
72. Hashemi, S.F., Mehrabi, M., Ehterami, A., Gharravi, A.M., Bitaraf, F.S. and Salehi, M., "In-vitro and in-vivo studies of pla/pcl/gelatin composite scaffold containing ascorbic acid for bone regeneration", ***Journal of Drug Delivery Science and Technology***, Vol. 61, (2021), 102077. https://doi.org/10.1016/j.jddst.2020.102077
73. Rozila, I., Azari, P., Munirah, S.b., Safwani, W.K.Z.W., Pingguan-Murphy, B. and Chua, K.H., "Polycaprolactone-based scaffolds facilitates osteogenic differentiation of human adipose-derived stem cells in a co-culture system", ***Polymers***, Vol. 13, No. 4, (2021), 597. https://doi.org/10.3390/polym13040597
74. Du, X., Yu, B., Pei, P., Ding, H., Yu, B. and Zhu, Y., "3d printing of pearl/caso 4 composite scaffolds for bone regeneration", ***Journal of Materials Chemistry B***, Vol. 6, No. 3, (2018), 499-509. https://doi.org/10.1039/c7tb02667f

Persian Abstract

**چکیده**

نقایص شایع استخوانی بزرگ معمولا به خودی خود خوب نمی شوند و کمپلکس ژلاتین/کیتوسان یکی از بهترین ترکیبات برای مهندسی بافت استخوان است، اما تجزیه سریع در محلول آبی و خواص مکانیکی کم نیاز به پیوند عرضی را افزایش می دهد. غلظت پیوند عرضی و روش پیوند عرضی بر خواص داربست ها تأثیر زیادی دارند. در اینجا، سه روش مختلف پیوند عرضی با گلوتارآلدئید (GA)، افزودن به محلول، قرار گرفتن در معرض بخار و غوطه وری با آنالیزهای مختلف برای یافتن بهترین تکنیک و غلظت مورد مطالعه قرار گرفتند. میکروسکوپ الکترونی روبشی ریزساختار متخلخل همگن را در تمامی نمونه ها نشان داد. درصد تورم و زیست تخریب پذیری با افزایش غلظت و زمان پیوند عرضی کاهش یافت اما خواص مکانیکی بهبود یافته است، همچنین تاثیر زمان نسبت به غلظت بیشتر بوده است. داربست پیوند داده شده با روش افزودن به محلول ( 1 wt .%) عملکرد بهتری نسبت به سایر نمونه ها داشته است و از خود زاویه تماس ۳۹/۳°، استحکام فشاری ۱/٤٥±۰/۰٥ مگاپاسکال، درصد تورم ۱/۳±۲۲/۳۱ (٪) و زیست تخریب پذیری ٤/٤۷±۲٦/۳۳ (٪)نشان داد. همچنین این نمونه زنده مانی سلولی بالاتر از ۸۰ (٪)داشته است و بیان آلکالین فسفاتاز (ALP) و استئوژن ها در طی ١٤ روز انکوباسیون سلولی بهبود یافته است که نشان دهنده ی ظرفیت بالای این نمونه در تمایز استخوانی می باشد. بنابراین این داربست به عنوان بهترین کاندید برای ترمیم استخوان و مطالعات بیشتر مهندسی بافت استخوان پیشنهاد می شود.